Journal of Solid State Chemistry 186 (2012) 81–86

Contents lists available at SciVerse ScienceDirect

Journal of Solid State Chemistry

journal homepage: www.elsevier.com/locate/jssc

Electronic structure and chemical bonding of α- and β-$CeIr_2Si_2$ intermediate valence compounds

Samir F. Matar [a,*], Rainer Pöttgen [b], Bernard Chevalier [a]

[a] CNRS, Université de Bordeaux, ICMCB, 87 Avenue du Docteur Albert Schweitzer, 33600 Pessac, France
[b] Institut für Anorganische Universität Münster, Corrensstrasse 30, D-48149 Münster, Germany

ARTICLE INFO

Article history:
Received 19 September 2011
Received in revised form
21 November 2011
Accepted 26 November 2011
Available online 4 December 2011

Keywords:
Intermetallic compounds
$CeIr_2Si_2$
Electronic structure
Equation of state
Dimorphism

ABSTRACT

The dimorphism of the intermediate valence ternary cerium silicide $CeIr_2Si_2$ in the $ThCr_2Si_2$ (α) and $CaBe_2Ge_2$ (β) modifications is addressed in the framework of the density functional theory. The geometry optimization is in good agreement with the experiment and the subsequent establishment of the energy–volume equation of state (EOS) indicates a stabilization of the β-type relative to the α-type concomitant with the trend of the cerium valence, changing to tetravalent in β-$CeIr_2Si_2$. This is equally shown from the site projected DOS and from the large increase of the electronic contribution to the specific heat. The chemical bonding indicates the strongest bonding interactions within the Ir–Si substructure in both varieties. Stabilization of β-$CeIr_2Si_2$ with almost tetravalent cerium is in good agreement with $Th^{IV}Ir_2Si_2$ which exclusively crystallizes in the $CaBe_2Ge_2$ type. The EOS behavior of different RIr_2Si_2 ($R=$Th, Ce, La) is comparatively discussed.

1. Introduction

Among the huge number of rare earth (*Ln*)-based intermetallic compounds, those with structures that are derived from the tetragonal $BaAl_4$ type [1] comprise one of the largest families [2,3]. These phases have intensively been studied in the last 40 years by solid state chemists and physicists with respect to their broadly varying physical properties [4] and this research topic recently gained a true renaissance, when superconductivity at $T_{max}=38$ K was observed for the solid solution $Ba_{1-x}K_xFe_2As_2$ [5,6].

The two simplest ternary substitution variants of the $BaAl_4$ structure are the $ThCr_2Si_2$ [7] and $CaBe_2Ge_2$ [8] types, where the chromium and silicon, respectively, beryllium and germanium atoms are ordered in two different manners on the aluminum substructure (Fig. 1). Besides these two structure types with almost 1000 representatives [3], diverse other substitution and distortion variants have been reported [9,10], which derive from the aristotype $BaAl_4$ via group–subgroup relations.

A very interesting phenomenon in the series $LnIr_2Si_2$ and $LnNi_2As_2$ is the occurrence of temperature driven dimorphism with a $ThCr_2Si_2$ type low- and $CaBe_2Ge_2$ type high-temperature modification [11]. Since the phase transition is of a reconstructive type, both modifications can be characterized under ambient conditions. This is especially interesting for cerium, europium, and ytterbium containing compounds, since for these materials valence changes and drastic differences in the physical properties can be expected.

Such temperature driven dimorphism occurs for the ternary silicide $CeIr_2Si_2$ [11]. β-$CeIr_2Si_2$ crystallizes directly from the melt, while α-$CeIr_2Si_2$ forms after annealing at 870 K [12,13]. The modifications of this compound have intensively been studied with respect to the magnetic and electrical properties [12,14–20]. Thermal expansion measurements show large hysteresis for the phase transition [20]. Temperature dependent magnetic susceptibility measurements and cerium XL_{III} absorption edges at 300 K [12,18] show that both modifications remain paramagnetic down to low temperature and reveal intermediate cerium valence. At room temperature α-$CeIr_2Si_2$ has a cerium valence of 3.32, while β-$CeIr_2Si_2$ tends towards tetravalent cerium with a value of 3.56 [12]. The intermediate cerium valence expresses itself in the course of the cell volumes in the $LnIr_2Si_2$ series. The $CeIr_2Si_2$ cell volumes are close or even smaller than those of $PrIr_2Si_2$. Also the intermediate cerium valence seems to weaken the overall chemical bonding. This is nicely reflected in the course of the phase transition temperatures which is the lowest one for the cerium compound in the series $LnIr_2Si_2$ ($Ln=$La, Ce, Pr, Nd) [20].

On the theoretical side, several works were devoted to the calculated electronic structure of intermetallic compounds with 1:2:2 stoichiometry such as the early study of the bonding in $ThCr_2Si_2$ and $CaBe_2Ge_2$ type main group solids by Zheng [21], $SrPt_2As_2$ [22] and dimorphism effects in YIr_2Si_2 [23] and $LaIr_2Si_2$ [24].

---

* Corresponding author. Fax: +33 5 4000 27 61.
E-mail addresses: matar@icmcb-bordeaux.cnrs.fr (S.F. Matar), pottgen@uni-muenster.de (R. Pöttgen), chevalie@icmcb-bordeaux.cnrs.fr (B. Chevalier).

0022-4596/$ - see front matter © 2011 Elsevier Inc. All rights reserved.
doi:10.1016/j.jssc.2011.11.041

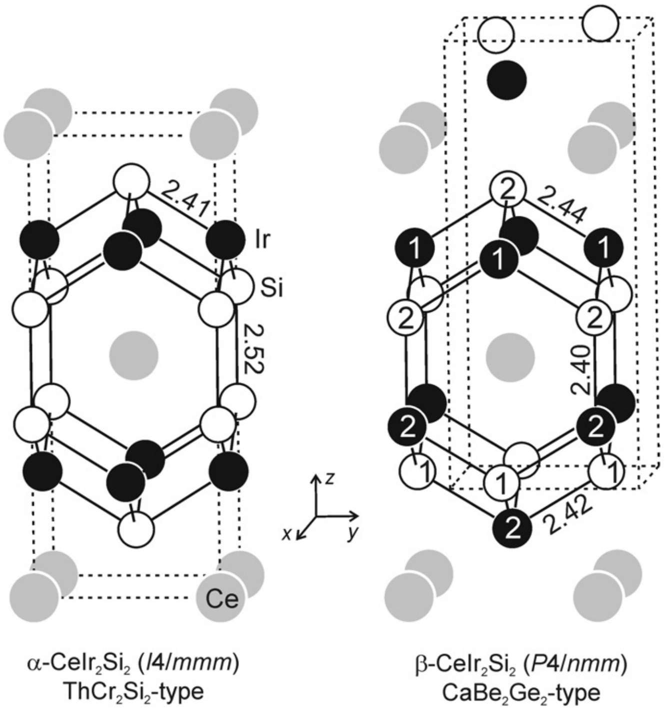

α-$CeIr_2Si_2$ (*I*4/*mmm*)
$ThCr_2Si_2$-type

β-$CeIr_2Si_2$ (*P*4/*nmm*)
$CaBe_2Ge_2$-type

Fig. 1. The crystal structures of α- and β-$CeIr_2Si_2$. Relevant interatomic distances (Å), the three-dimensional [Ir_2Si_2] networks and the crystallographically independent iridium and silicon sites are indicated.

Although both modifications of $CeIr_2Si_2$ have intensively been studied with respect to their magnetic, electrical and thermal expansion behavior, the electronic structure and chemical bonding have not been investigated. In the course of our systematic studies of chemical bonding in $Ce_xIr_yX_z$ intermetallics [25–29] we have now studied α- and β-$CeIr_2Si_2$ by *ab initio* electronic structure calculations within the well established quantum theory framework of the density functional theory (DFT) [30,31]. $CeIr_2Si_2$ is one of the rare intermetallic cerium compounds exhibiting a valence change that is accompanied by a switch in crystal structure, making it a model compound for the investigations of crystal structure–property and electronic structure–property relationships.

2. Crystal chemistry

The structures of α- and β-$CeIr_2Si_2$, as obtained from single crystal diffractometer data [13] are presented in Fig. 1. The cerium atoms in both modifications have coordination number 16 by 8 Ir+8 Si atoms. As emphasized in Fig. 1, due to the different coloring of iridium and silicon on the aluminum substructure of $BaAl_4$, the range in Ce–Ir and Ce–Si distances is different in both modifications. While the Ce–Si distances (8×3.155 Å in α-$CeIr_2Si_2$; 4×3.180 and 4×3.181 Å in β-$CeIr_2Si_2$) are almost similar, the Ce–Ir distances (8×3.262 Å in α-$CeIr_2Si_2$; 4×3.155 and 4×3.260 Å in β-$CeIr_2Si_2$) are distinctly different. The shorter Ce–Ir distances in β-$CeIr_2Si_2$ are a consequence of the almost tetravalent character of cerium, strengthening the Ce–Ir bonding. Such behavior has repeatedly been observed in diverse $Ce_xRu_yX_z$ (X=Mg, Cd, Al, In, Sn) intermetallics [32,33] with intermediate cerium valence and short Ce–Ru bonds.

Together Ir and Si atoms build up a three-dimensional [Ir_2Si_2] network in both modifications. The Ir–Si distances range from 2.41 to 2.44 Å, in good agreement with the sum of the covalent radii [34] of 2.44 Å, indicating substantial Ir–Si bonding. This is addressed in more detail in the chemical bonding section (*vide infra*). While no direct Si–Si contacts are observed in β-$CeIr_2Si_2$, Si_2 pairs with 2.52 Å Si–Si distance occur in α-$CeIr_2Si_2$. These distances are much longer than in the diamond modification of silicon (2.35 Å) [35].

Although the shortest Ce–Ce distances in both modifications (4.09 Å in α-$CeIr_2Si_2$ and 4.15 Å in β-$CeIr_2Si_2$) are well above the Hill limit for *f* electron localization [36], one observes non-integer cerium valence. For further crystal chemical details on α- and β-$CeIr_2Si_2$ we refer to the original crystallographic work [13]. In the following sections we focus on the electronic structure and chemical bonding in this fascinating silicide.

3. Computational details

Within DFT we use two complementary computational methods. The Vienna *ab initio* simulation package (VASP) code [37,38] allows geometry optimization and subsequent establishment of the energy–volume equations of states for the α and β forms of $CeIr_2Si_2$. For this we use the projector augmented wave (PAW) method [39] (particularly accurate for studying rare earths), built within the generalized gradient approximation (GGA) scheme following Perdew, Burke and Ernzerhof (PBE) [40]. The conjugate-gradient algorithm [41] is used in this computational scheme to relax the atoms of the different crystal setups. The tetrahedron method with Blöchl corrections [39] as well as a Methfessel–Paxton [42] scheme were applied for both geometry relaxation and total energy calculations. Brillouin-zone (BZ) integrals were approximated using the special *k*-point sampling of Monkhorst and Pack [43]. The optimization of the structural parameters was performed until the forces on the atoms were less than 0.02 eV/Å and all stress components less than 0.003 eV/Å^3. The calculations are converged at an energy cut-off of 273 eV for the plane-wave basis set with respect to the *k*-point integration with a starting mesh of $4 \times 4 \times 4$ up to $8 \times 8 \times 8$ for best convergence and relaxation to zero strains. Then all-electron calculations, equally based on the DFT with GGA-PBE functional [40], are carried out for a full description of the electronic structure and the properties of chemical bonding. They are performed using the full potential scalar-relativistic augmented spherical wave (ASW) method [44]. In the ASW method, the wave function is expanded in atom-centered augmented spherical waves, which are Hankel functions and numerical solutions of Schrödinger's equation, respectively, outside and inside the so-called augmentation spheres. In the minimal ASW basis set, we chose the outermost shells to represent the valence states and the matrix elements were constructed using partial waves up to $l_{\max}+1=4$ for Ce, i.e., 4*f* states were considered within the basis set, $l_{\max}+1=3$ for Ir and $l_{\max}+1=2$ for Si. Self-consistency was achieved when charge transfers and energy changes between two successive cycles were such as: $\Delta Q < 10^{-8}$ and $\Delta E < 10^{-6}$ eV, respectively. The Brillouin zone integrations were performed using the linear tetrahedron method within the irreducible wedge [39]. The calculations were carried out assuming spin degenerate configuration. Besides the site projected density of states, we discuss qualitatively the pair interactions based on the overlap population analysis with the crystal orbital overlap population (COOP) [45]. In the plots, positive, negative, and zero COOP magnitudes indicate bonding, anti-bonding, and non-bonding interactions, respectively. Here we use the integrated *i*COOP criterion to address relative bonding intensities. We note that another scheme for describing the chemical bonding, the ECOV (covalent bond energy) criterion based on both the overlap and the Hamiltonian populations is also accessible within the ASW method [44]. It provides similar qualitative results to the COOP but tends to exaggerate the intensity of the ECOV involving *f* states.